EFFECT OF ANNEALING ON MICROSTRUCTURE AND CORROSION PERFORMANCE OF ADB AND ALB ALLOYS

M. Mohammadnejad, M. Ehteshamzadeh* and S. Soroushian

* *ehtesham@uk.ac.ir*

Received: July 2013 **Accepted: March 2014**

Department of Materials Science and Engineering, Faculty of Engineering, Shahid Bahonar University of Kerman, Iran.

Abstract: *Microstructure and corrosion performance of admiralty brass (ADB) and aluminum brass (ALB) alloys after passing different annealing heat treatments were investigated using optical and scanning electron microscope, energy dispersive X-ray spectroscopy (EDS), X-ray diffraction (XRD), DC polarization measurements and electrochemical impedance spectroscopy (EIS). The results showed that heat treating of ALB caused gradient in aluminum concentration across the grains whose increased with increasing of annealing temperature. On the other hand, corrosion current density (i_{corr}) of ADB in 3.5%NaCl media decreased with increasing of recrystallization, while ALB showed corrosion behavior inconsistent with ADB. The impedance measurements showed that corrosion rate of ADB decreased with increasing of exposure time from 0 to 15 days which could be related to the formation of SnO_2 surface film and the Sn-rich phases. While polarization resistance of ALB decreased by passing days in the corrosive media which could be associated to establishing of differential aluminum concentration cells.*

Keywords: *Admiralty brass, Aluminum brass, Annealing, Microstructure, Corrosion resistance.*

1. INTRODUCTION

Brass alloys have good or poor cold working behavior depending on the amount of Zn in the alloy. Typically, brass alloys with low Zn contents have good or excellent cold working characteristics, while brasses with high Zn contents have poor cold working qualities [1]. Among the brasses, admiralty brass (ADB) and aluminum brass (ALB) alloys have been used extensively in water distribution systems, water treatment units, condensers and heat exchangers. However, pitting corrosion, dezincification and stress corrosion cracking of brasses are problematic phenomena in water that have been widely studied till now [2-7]. During the past decade, many techniques have been used to minimize the dezincification and corrosion of brasses, one of which is alloying. Trace addition of alloying elements like arsenic, boron and nickel have been used to improve the dezincification resistance of Al-brass in various aggressive environments [8, 9]. On the other hands, Copper alloys containing 20–40% Zn are highly susceptible to stress-corrosion cracking which can be controlled and prevented in two ways: by selecting an alloy with high resistance to the phenomena (i.e. an alloy with low Zn content) and by reducing residual stresses by annealing about 250°C, which should not affect the mechanical properties of the material [1]. Also, electrochemical behavior of brasses under stagnant and stirring conditions specially in corrosive media containing Cl^- have been widely studied as well as their microstructure and mechanical properties [2, 7, 10-14]. However, very little work has been directed to study the electrochemical behavior and corrosion performance of admiralty and aluminum brasses after annealing at temperatures that affects the microstructure.

The aim of the present study was to investigate the effect of relatively high temperatures annealing treatments on microstructure and corrosion performance of ADB and ALB alloys.

2. EXPERIMENTAL PROCEDURE

2. 1. Materials, Methods and Heat Treatments

ADB and ALB specimens with chemical composition given in Table 1 were taken from commercial plates produced by extrusion and drawing processes in Shahid Bahonar Copper

Table 1. Chemical composition (wt%) of the admiralty brass and aluminum brass alloys

	Sn	Pb	Fe	Mn	Al	Zn	Cu
ADB	0.97	0.01	0.038	0.38	0.001	25.86	73.12
ALB	~0	0.01	0.018	0.38	1.80	18.05	80.09

Industries company. The drawn specimens were annealed at 630, 700 and 780 °C for 60 and 120 minutes in an annealing furnace with argon atmosphere. Then, the specimens were polished with successive grades of SiC emery papers from 400 to 3000 grit numbers to achieve mirror finishing. For microstructure studies, the specimens were washed with double distilled water and then with acetone and etched in 28%HNO_3+42% CH_3COOH+30% H_2O solution. Electrochemical specimens were prepared by mounting the squared specimens with dimensions of 1cm 1cm in polyester after soldering a copper wire suitably on the surface.

2. 2. Electrochemical Measurements

Electrochemical studies were carried out using potentiostat/Galvanostat model 263A EG&G Princeton Applied Research (PAR) using a three electrodes cell with a platinum electrode as counter electrode, saturated calomel electrode (SCE) as reference electrode and the samples with an exposed area of 1 cm^2 as working electrode. 3.5% NaCl aqueous solution was used as the corrosive media. Potentiodynamic polarization curves were recorded by scan rate of 1mV/s in the potential range of ±250 mV versus open circuit potential (OCP). Electrochemical impedance spectroscopy (EIS) measurements were completed in the frequency range of 100kHz–10mHz with five points per decade and sinusoidal wave amplitude of 10mV. Corrosion parameters were extracted from polarization and EIS plots [15]. Polarization curves were analyzed using "Softcorr 352" software by Tafel extrapolation (linear parts of anodic and cathodic branches) technique. The spectra of EIS were modeled with an equivalent circuit proposing with "Zview" software according to the electrochemical phenomena. All of the electrochemical Data were recorded after 90 minutes for stabilizing of conditions.

2. 3. Characterization of the Corrosion Products and Microstructure

The microstructure of the samples was observed by an OLYMPUS optical microscope and CamScan 2300 MV scanning electron microscope equipped with energy dispersive X-ray spectroscopy (EDS). For X-ray diffraction analysis a Philips X'pert difractometer (XRD) using Cu Kα radiation was employed for detection of the phases formed on the alloys surfaces immediately after completing electrochemical tests. The spectra were analyzed by "X'Pert High sore 1.0d" software.

3. RESULTS AND DISCUSSION

3. 1. Microstructure

Fig. 1 shows the microstructures of the annealed admiralty brass alloy specimens. It was found that annealing at 630°C for 60 minutes could not cause an obvious change in fibrous microstructure. However, a small number of recrystallized grains uniformly distributed between tortuous fibrous grains interface were observed (Fig. 1a). This means that nucleation and growth of recrystallized grains were dominantly restricted inside the original fibrous grains. In this case the most boundaries of the new grains failed to migrate across the original grain interfaces. It seems that these time and temperature of annealing could not provide sufficient kinetic energy for recrystallization [16]. Stronger recrystallization was observed after annealing at 630 °C for 120 minutes or 700°C for 60 minutes which resulted in obviously squiggly interfaces and local breaking

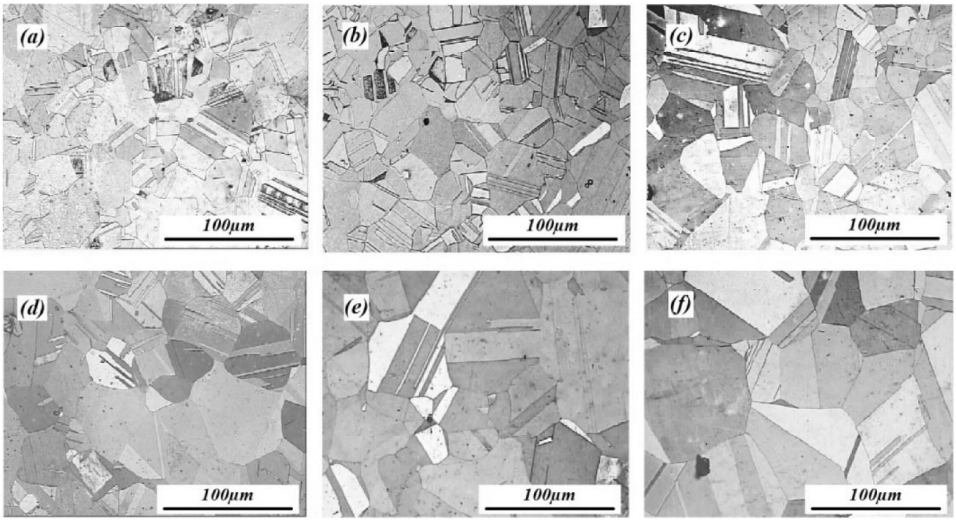

Fig. 1. Optical micrographs of annealed a dmiralty brass alloy specimens annealed at (a) 630°C for 60min, (b) 630°C for 120min, (c) 700°C for 60min, (d) 700°C for 120min, (e) 780°C for 60min, (f) 780°C for 120 min.

of the elongated fibrous microstructure (Fig. 1b and 1c). Increasing of the annealing temperature and time caused gradually augmentation of the recrystallization and disappearing of the fibrous microstructure (Fig. 1d and 1e). Wide-ranging recrystallization was arrived by annealing at 780°C for 120 minutes (Fig. 1f). Figure 2 shows typical SEM micrographs of aluminum brass annealed at 630 °C and 780 °C for 120 minutes. Table 2 lists EDS analysis of four different points (tip of the arrows) in different positions from the center to the grain boundaries. The results are also illustrated in Fig. 3. It's obvious that aluminum concentration gradient in the grains increased with increasing of annealing temperature.

Table 2. EDS analysis of aluminum brass alloys annealed at (a) 630°C and (b) 780°C for 120 minutes according to the positions showed in Fig. 2..

Annealing conditions	positions	Cu (wt%)	Zn (wt%)	Al (wt%)
630°C for 120 min	Spectrum 1	78.55	19.90	1.55
	Spectrum 2	78.76	19.96	1.28
	Spectrum 3	80.27	19.01	0.72
	Spectrum 4	80.27	19.01	0.72
780°C for 120 min	Spectrum 1	79.77	18.08	2.15
	Spectrum 2	79.28	18.98	1.74
	Spectrum 3	81.45	18	0.55
	Spectrum 4	80.78	18.79	0.43

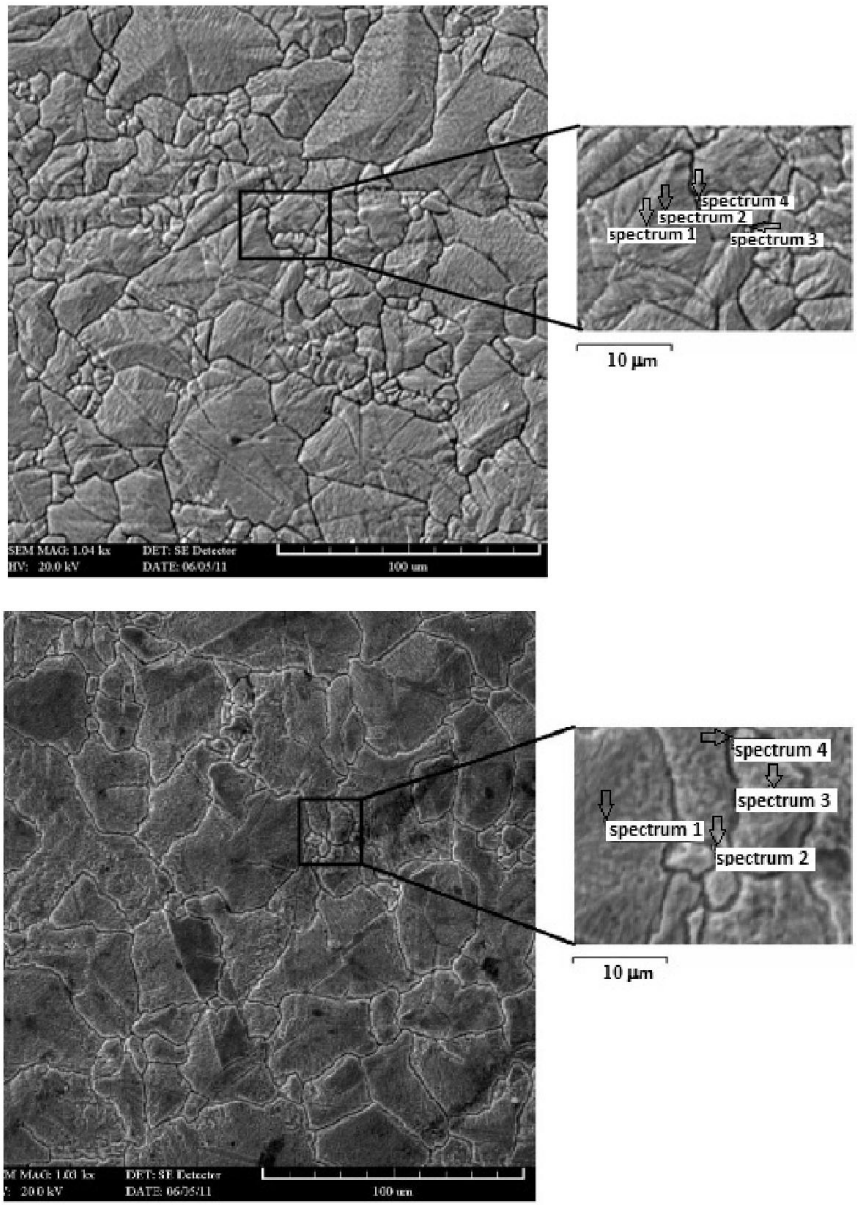

Fig. 2. Typical SEM micrographs of aluminum brass annealed at (a) 630°C and (b) 780°C for 120 minutes.

3. 2. Polarization Studies

Fig. 4 shows the polarization curves of admiralty and aluminum brass alloys specimens annealed at different temperatures and times. Increasing of annealing temperature and time in heat treatment of ADB shifted corrosion potential (E_{corr}) to more positive values and decreased corrosion current density (i_{corr}) in the active region. Polarization parameters are disclosed in Table 3 containing the values of corrosion

Table 3. Polarization parameters of ADB in 3.5% NaCl solution after annealing at different times and temperatures

Temperature (°C)	Time (minutes)	E_{corr} (V)	i_{corr} (A/cm^2)
630	60	-0.278	3.06×10^{-6}
	120	-0.280	2.77×10^{-6}
700	60	-0.233	1.84×10^{-6}
	120	-0.229	1.63×10^{-6}
780	60	-0.204	3.98×10^{-7}
	120	-0.192	1.32×10^{-7}

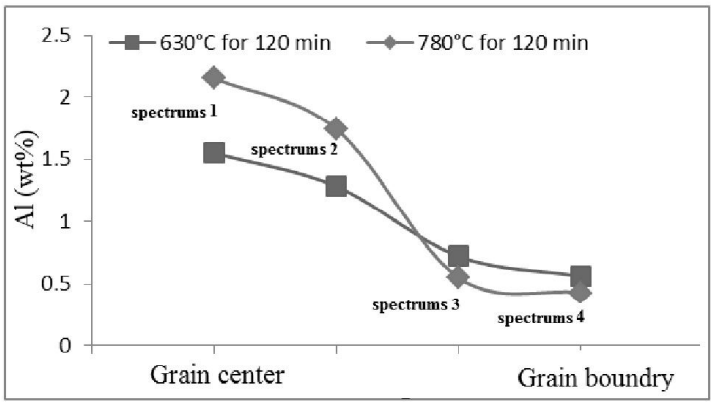

Fig. 3. EDS results in different points presented in Fig. 3 for aluminum brass annealed at 630°C and 780°C for 120 minutes.

potentials and corrosion current densities in different annealing temperatures and times. The admiralty brass specimens annealed at 780°C for 120 minutes possessed the highest corrosion resistance. But a counter behavior was observed in ALB whose could be related to aluminum concentration gradient (Fig. 3) that was encouraged in higher temperatures and longer times of heat treatment. It has been reported [12] that in the potential range of ±250 mV versus open circuit potential, there are two peaks in the current densities of anodic branch. The first one could be related to the formation of Cu_2O according to the following equations:

$$Cu+OH^- \leftrightarrow Cu(OH)_{(ads)}+e^- \quad (1)$$

$$2Cu(OH)_{(ads)} \leftrightarrow Cu_2O+H_2O \quad (2)$$

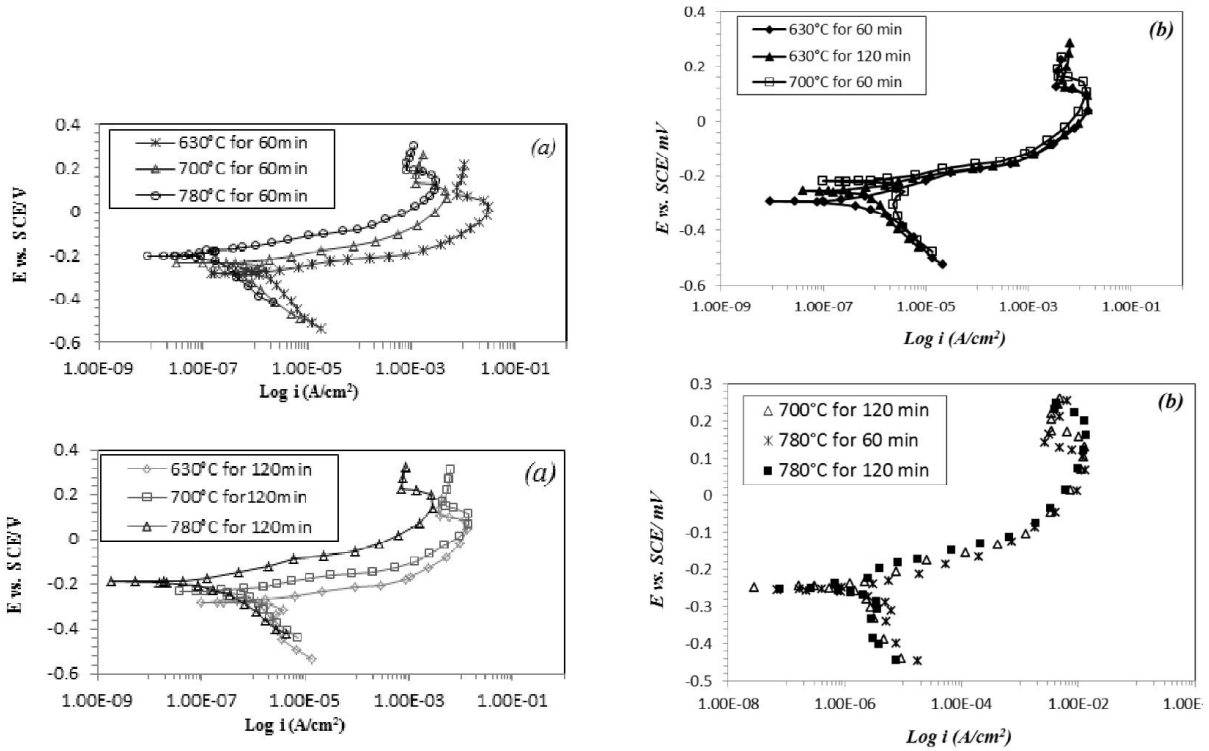

Fig. 4. Polarization curves of the alloys in 3.5% NaCl solution after different annealing temperatures and times: (a) ADB, (b) ALB.

The second anodic current density peak corresponds to formation of CuCl salt layer. This layer is mainly a result of a combined dissolution reaction. This involves the electrochemical adsorption of Cl^-:

$$Cu+Cl^- \leftrightarrow CuCl_{(ads)}+e^- \quad (3)$$

followed by chemical dissolution:

$$CuCl_{(ads)}+Cl^- \leftrightarrow CuCl_2^- \quad (4)$$

or chemical adsorption of Cl :

$$Cu(OH)_{(ads)}+Cl^- \leftrightarrow CuCl_{(ads)}+OH^- \quad (5)$$

3. 3. EIS Measurements

Fig. 5 presents Nyquist plots of ADB and ALB alloys in 3.5%NaCl solution after heat treated at different annealing temperatures and times. It is remarkable that for ADB, the highest polarization resistance belonged to the specimens annealed at 780°C for 120 minutes. Also, there was a good agreement between the results obtained from polarization and EIS techniques.

Fig. 6 shows EIS spectra recorded after 1, 3, 7, 10 and 15 days exposing in 3.5%NaCl solution. The effect of corrosion products formed on ADB and ALB alloys annealed at 780°C for 120 minutes is revealed by comparing the results. Polarization resistance of ADB specimens annealed at 780°C for 120 minutes increased with increasing of exposure time, which suggests an increase in the charge transfer resistance or the oxide film resistance. Nyquist plots of ADB (Fig. 6a) showed that the impedance of the alloy increased with increasing of immersion time, indicating formation of a protective film on the alloy surface.

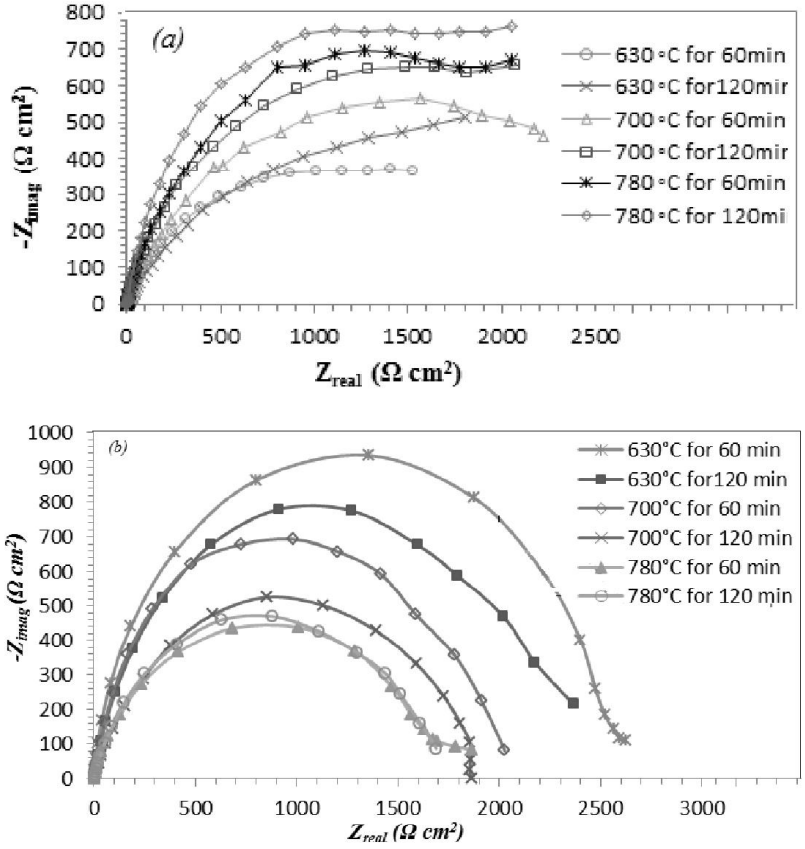

Fig. 5. Nyquist plots of the alloys in 3.5% NaCl media after different annealing temperatures and times: (a) ADB and (b) ALB.

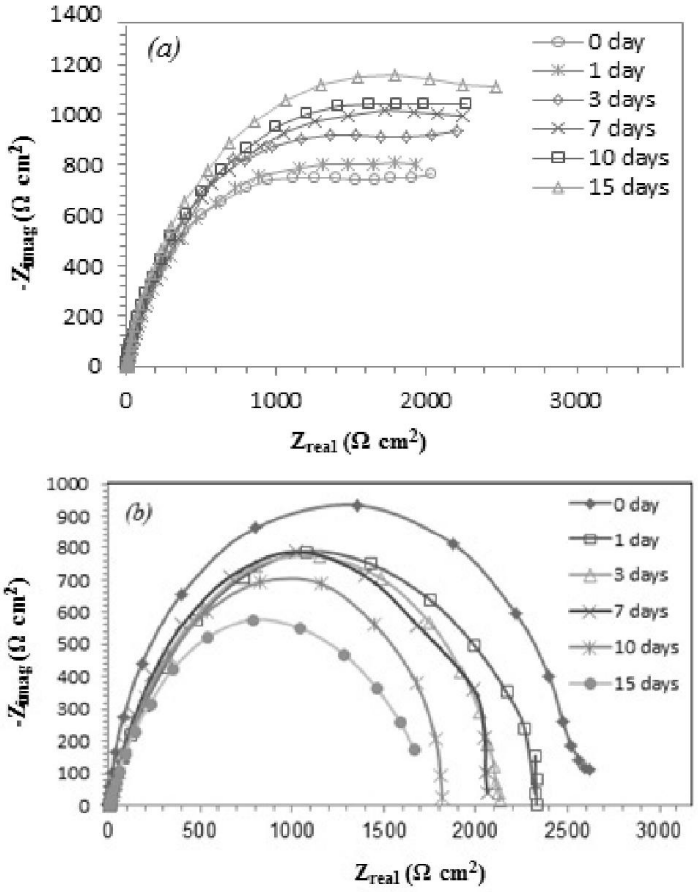

Fig. 6. Impedance spectra of the alloys annealed at 780°C for 120 min after exposing for 0, 1, 3, 7, 10 and 15 days in 3.5%NaCl solution: (a) ADB and (b) ALB.

Fig. 7 shows typical Bode and Bode-phase plots of ADB alloy annealed at 780°C for 120 min and exposed to 3.5 % NaCl solution for 0, 1 and 3 days. These plots acquired the concluding records for proposing the equivalent circuit for modelling of the impedance data. The impedance data were analyzed in terms of an equivalent circuit shown in Fig. 7, too. R_{ct} is charge transfer resistance, CPE is a constant phase element and R_s is resistance of the electrolyte and was very small (6.80–4.06Ω) because it was always tried to place the counter electrode against the working one in a nearly constant distance. There is one peak in the phase angle that could be associated to the capacitance part of the electrical circuit model [17-19].

CPE is a special element, whose value is a function of the angular frequency, ω, and whose phase is independent of the frequency. Its admittance and impedance components are defined as follows:

$$Y_{CPE}=Y_0(j\omega)^n \quad (1)$$

$$Z_{CPE}=1/[Y_0(j\omega)^n] \quad (2)$$

where, j is the imaginary number, $j=(-1)^{1/2}$ and $\omega=2\pi f$ is the angular frequency [19]. n is defined as surface roughness factor (ratio of apparent to real surface area) and is the CPE power, a parameter that lies between 0 and 1. For n = 1, the CPE describes an ideal capacitor with Y_0 equal to the capacitance C and for n = 0, the CPE is an ideal resistor. For $0.5 < n < 1$, the CPE describes a frequency dispersion of time constants due to local inhomogeneity on the surface [20-21].

Modelling of the experimental data by Zview software followed almost the same pattern and the inaccuracy did not exceeded 3%. Table 4 lists EIS parameters of ADB in 3.5% NaCl solution

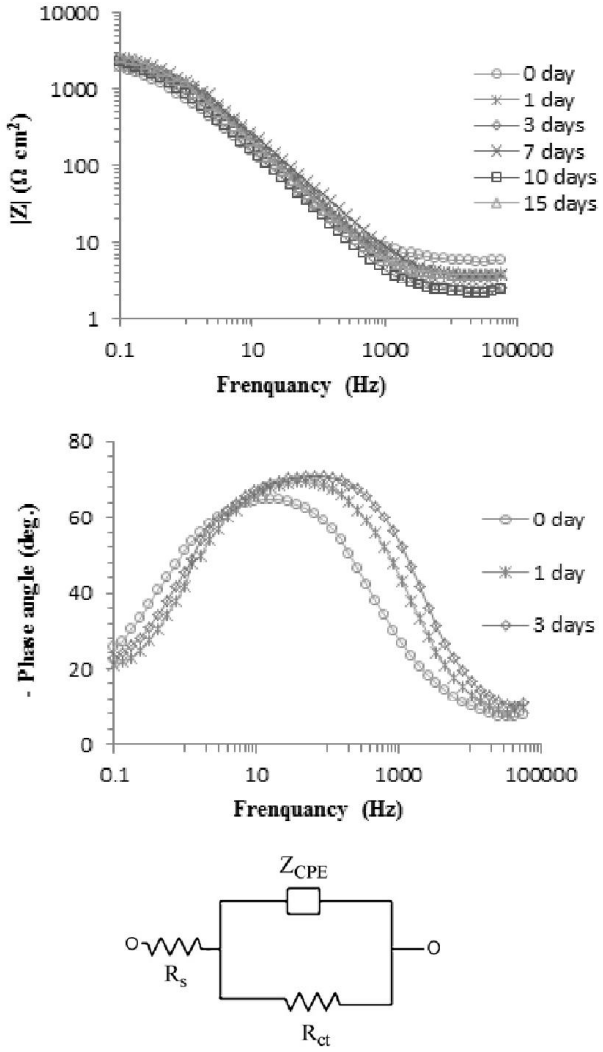

Fig. 7. Typical Bode and Bode-phase plots of ADB alloy annealed at 780°C for 120 min after 0, 1 and 3 days immersion in 3.5%NaCl solution for proposing of an equivalent circuit for modelling the impedance data. (Rs,resistance of the electrolyte; CPE, constant phase element of the electrical double layer (EDL); Rct, charge transfer resistance of the electrical double layer (EDL)).

after annealing at different times and temperatures whose experimental data were illustrated in Fig. 5. Also, Table 5 lists EIS parameters of ADB annealed at 780 °C for 120 min and exposed to 3.5% NaCl solution for different days whose experimental data were illustrated in Fig. 6. The results showed that charge transfer resistance increased with increasing of exposure time in the corrosive media which could be caused by formation of a protective film. Also, quantities of "n" in the admiralty brass alloy specimens are close to 0.8 and are physically interpreted to the capacitance of a rough surface. The impedance (Z) for the specimens annealed at 780 °C for 120 minutes increases from 2212 Ω cm² after immersion for 90 minutes to about 2984 Ω cm² after exposure of 15 days, due to the formation of the film. Fig. 8 shows the effect of annealing temperature on the polarization resistance of the ADB and ALB alloys in 3.5% NaCl. Annealing caused a counter effect on the corrosion performance of ADB and ALB. This could be related to the concentration gradient of the alloying elements as well as formation of intermetallic phases shown in Fig. 3, 9 and 10 (as follows) in ALB.

Table 4. EIS parameters of ADB in 3.5% NaCl solution after annealing at different times and temperatures

Temperature (°C)	Time (min)	$R_s(\Omega)$	$R_{ct}(\Omega)$	$Y_1(\Omega^{-1}S^n)$	n (0<n<1)
630	60	5.80	1362	34.87×10^{-5}	0.78
	120	6.17	1541	40.98×10^{-5}	0.70
700	60	4.44	1758	16.32×10^{-5}	0.79
	120	4.65	1970	24.22×10^{-5}	0.82
780	60	6.77	2045	12.90×10^{-5}	0.81
	120	6.80	2212	12.64×10^{-5}	0.80

Table 5. EIS parameters of ADB annealed at 780°C for 120 min and immersed in 3.5% NaCl solution for different exposure times

Immersion time	$R_s(\Omega)$	$R_{ct}(\Omega)$	$Y_1(\Omega^{-1}S^n)$	n (0<n<1)
0 day	6.80	2212	12.64×10^{-5}	0.80
1 day	5.74	2467	23.30×10^{-5}	0.76
3 days	4.39	2537	14.72×10^{-5}	0.82
7 days	5.34	2791	12.26×10^{-5}	0.77
10 days	4.06	2856	18.47×10^{-5}	0.80
15 days	5.68	2984	13.31×10^{-5}	0.82

3. 4. Surface Characterization Studies

Fig. 9(a) shows the X-ray diffraction patttern of ADB alloy annealed at 630°C and 780°C for 60 minutes. Several phases involving CuZn, Cu_3Sn, $Cu_{40}Sn_{11}$ and $Cu_{20}Sn_6$, were observed in the alloy annealed at 630°C for 60 minutes. XRD patterns of the samples annealed at 780°C for 60 minutes showed similar phases. However, the peaks of Cu_3Sn, $Cu_{40}Sn_{11}$ and $Cu_{20}Sn_6$ phases in the samples annealed at 780°C for 60 minutes showed more intensity than those found in the samples annealed at 630°C for the same duration. It is clear that formation of Sn-rich phases increased with increasing of annealing temperature and time.

Fig. 9(b) shows XRD patterns of the oxide scales formed on the surfaces of the admiralty brass alloy specimens annealed at 630°C and 780°C for 60 minutes after ten days exposed to 3.5%NaCl solution. Appearance of the substrate peaks in the XRD patterns origins from the fact that depth of penetration of X-ray is greater than thickness of the surface film. The peaks of SnO2 phase were observed on the surface film as corrosion products. Increasing of annealing temperature and time caused intensifying of the peaks related to SnO_2 in the sample annealed at 780°C for 60 minutes. This could be related to the growth of Sn-rich phases during heat treatment. According to the Pourbaix diagram of the Sn/H_2O system [22-23] and the surface characteristics of the Sn-containing copper alloys in the sodium chloride solution, the formation of SnO2 in this environment was proposed to proceed through the following reaction scheme:

$$Sn+4H_2O\rightarrow Sn(OH)_4+4e^-+4H^+ \quad (6)$$

Sn may also be oxidized according to the following reactions:

$$Sn+2H_2O\rightarrow Sn(OH)_2+2e^-+2H^+ \quad (7)$$

$$Sn(OH)_2+2H_2O\rightarrow Sn(OH)_4+2e^-+2H^+ \quad (8)$$

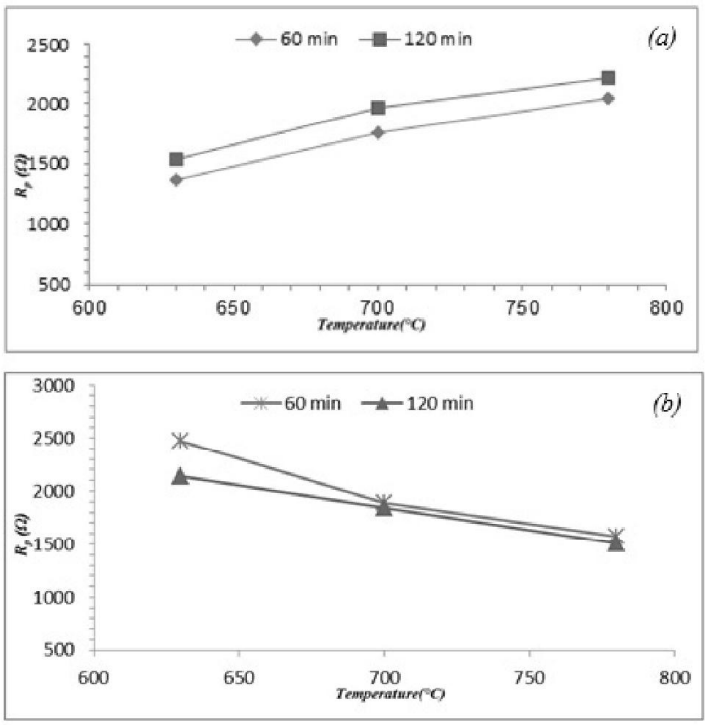

Fig. 8. Variation of polarization resistance versus temperature of annealing: (a) ADB alloy, (b) ALB alloy.

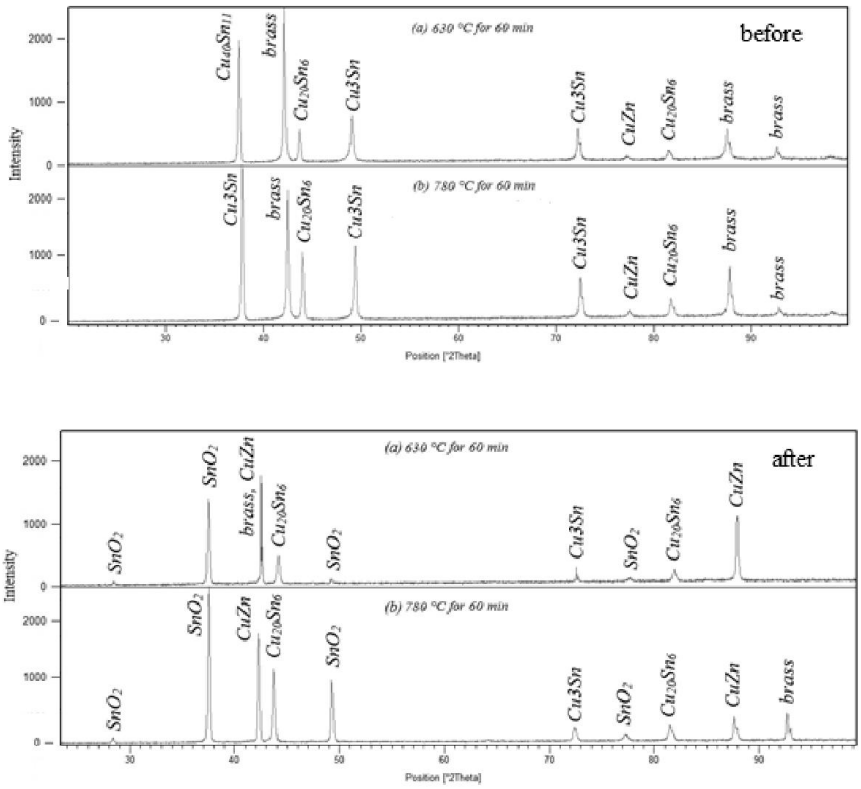

Fig. 9. XRD patterns of annealed ADB before and after ten days exposure to 3.5%NaCl solution: (a) 630°C for 60min (b) 780°C for 60min.

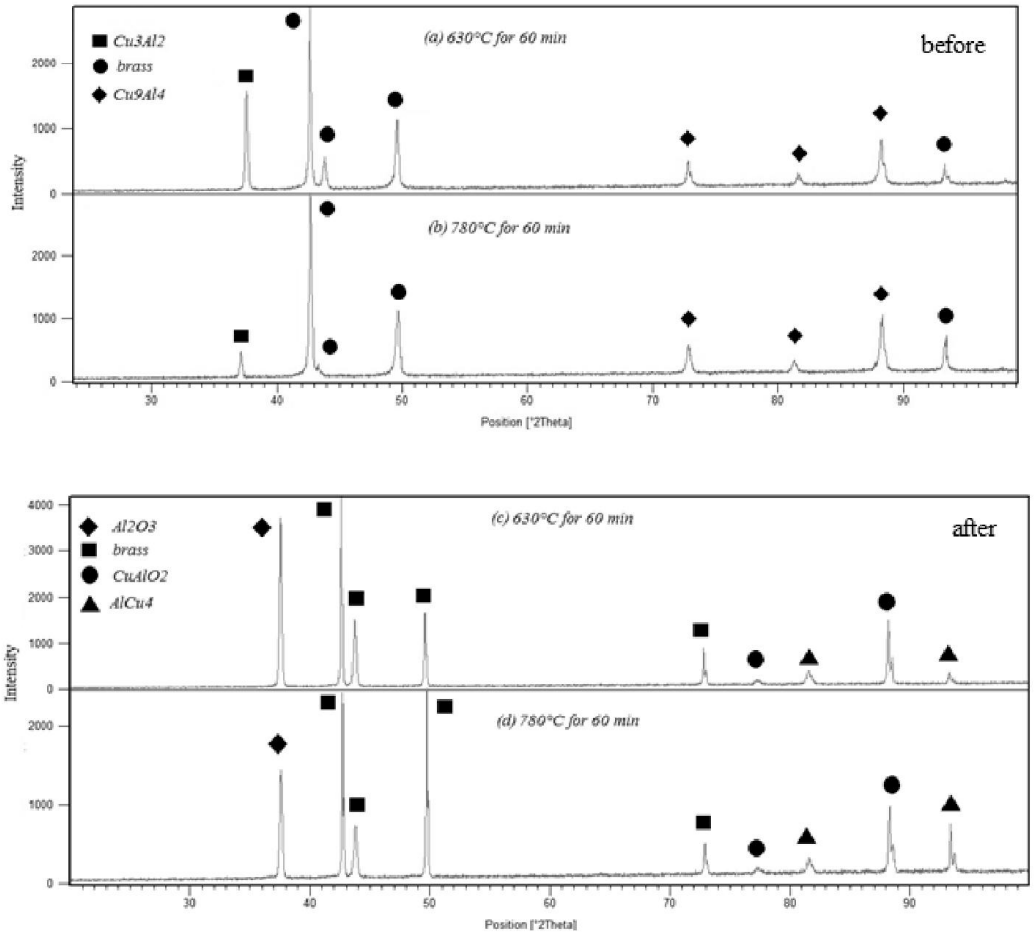

Fig. 10. XRD patterns of annealed ALB before and after ten days exposure to 3.5%NaCl solution: (a) 630°C for 60min (b) 780°C for 60min.

The following dehydration reaction can take place:

$$Sn(OH)_4 \rightarrow SnO_2 + 2H_2O \quad (9)$$

Therefore, the tendency of copper alloys to form SnO_2 oxide layer increases with increasing of Sn-rich phases.

Figures 10(a) and 10(b) show XRD patterns of ALB alloy before and after 10 days expoture to 3.5%NaCl solution. Decreasing of polarization resistance of ALB shown in Fig. 8 could be related to the formation of Al reach intermetallic phases as Cu_3Al_2 and Cu_9Al_4. These phases can provide anodic phases and sufficient electro motive force for electrochemical cells.

4. CONCLUSIONS

1. For ADB, increasing of annealing temperature and time caused disappearing of the fibrous microstructure gradually and encouragement of recrystallization. In addition, Sn-rich sub-grains were formed in the annealing process.
2. Corrosion resistance of ADB was improved with increasing of annealing temperature and time and so the alloy annealed at 780°C for 120 minutes showed the highest corrosion resistance in 3.5%NaCl solution.
3. Also, Corrosion rates of ADB decreased after 10 days exposing to 3.5%NaCl solution that was related to the formation of Sn-rich oxide film on the surface of the alloy.

4. Increasing of annealing temperature caused declining of corrosion resistance of ALB which could be interpreted as the result of strong aluminum concentration gradient across the grains and establishing of differential aluminum concentration cells.
5. Corrosion rate of ALB increased after 10 days exposure to 3.5%NaCl solution which might be related to establishing of galvanic cells as the result of formation of intermetallic phases such as $CuAl_4$ as well as differential aluminum concentration cell.

REFERENCES

1. Pola, A., Gelfi, M., Eleonora Depero and L., Roberti, R., "Study of annealing temperature effect on stress-corrosion cracking of aluminum brass heat-exchangers tubes by microdiffraction experiments", Engineering Failure Analysis, 2008, 15, 54–61.
2. Alfantazi, A. M., Ahmed, T. M. and Tromans, D., "Corrosion behavior of copper alloys in chloride media", Materials and Design, 2009, 30, 2425–2430.
3. Sayed, S. M., Ashour, E. A. and Youssef, G. I., "Effect of sulfide ions on the corrosion behaviour of Al–brass and Cu10Ni alloys in salt water, Materials Chemistry and Physics", 2003, 78, 825–834.
4. Rahmouni, K., Keddam, M., Srhiri, A., Takenouti, H., "Corrosion of copper in 3% NaCl solution polluted by sulphide ions", Corrosion Science, 2005, 47, 3249–3266.
5. Milosev, I., "The effect of various halide ions on the passivity of Cu, Zn and Cu–xZn alloys in borate buffer", Corrosion Science, 2007,49, 637–653.
6. Polunin, A. V., Pchelnikov, A. P., Losev, V. V. and Marshakov, I. K., "Electrochemical studies of the kinetics and mechanism of brass dezincification", Electrochimica Acta., 1982, 27, 467–475
7. Dinnappa, R. K., Mayanna, S. M., "The dezincification of brass and its inhibition in acidic chloride and sulphate solutions", Corrosion Science, 1987, 27, 349–361.
8. Chen, J. L., Li, Z. and Zhao, Y. Y., "Corrosion characteristic of Ce Al brass in comparison with As Al brass", Materials and Design, 2009, 30, 1743–1747.
9. Campanella, L., ColacicchiAlessandri, O., Ferretti, M. and Plattner, S. H., "The effect of tin on dezincification of archaeological copper alloys", Corrosion Science, 2009, 51, 2183–2191.
10. Gaoyong, L., Yuxiong, Z., Juhua, Z., Yanming, Z., Jian, L. and Liping, S., "Influence of rare earth elements on corrosion behavior of Al-brass in marine water", Journal of Rare Earths, 2011, 29, 638-644.
11. Habib, K., Riad, W., Muhanna, K., Al-Sumait, H., "Electrochemical behavior of Al-brass in polluted natural seawater", Desalination, 2002, 142, 5-9.
12. Osman, M. M., "Corrosion inhibition of aluminium–brass in 3.5% NaCl solution and sea water, Materials Chemistry and Physics", 2001, 71, 12–16.
13. El-Sherif, M., Ismail, M. and Badawy, A., "Effect of Zn and Pb as alloying elements on the electrochemicalbehavior of brass in NaCl solutions", Electrochimica Acta, 2004, 49, 5139–5150.
14. Sohn, S. and Kang, T., "The effects of tin and nickel on the corrosion behavior of 60Cu–40Zn alloys", Journal of Alloys and Compounds, 2002, 335, 281–289.
15. Stansbury, E. and Buchanan, R., "Fundamentals of Electrochemical Corrosion, ASM International", 1998, 248.
16. Mao, X., Fang, F., Yang, F., Jiang, J. and Tan, R., "Effect of annealing on microstructure and properties of Cu–30Ni alloy tube.", Journal of Materials Processing Technology, 2009, 209, 2145–2151.
17. Yuan, S. J. and Pehkonen, S. O., "Surface characterization and corrosion behavior of 70/30 Cu–Ni alloy in pristine and sulfide-containing simulated seawater", Corrosion Science, 2007, 49, 1276–1304.
18. Zhou, X. Zh., Deng, Ch. P. and Su, Y. Ch., "Comparative study on the electrochemical performance of the Cu–30Ni and Cu–20Zn–10Ni alloys", Journal of Alloys and Compounds, 2010, 491, 92-97.
19. Farzaneh, A., Ehteshamzadeh, M. and Mohammadi, M., "Corrosion performance of

the electroless Ni–P coatings prepared in different conditions and optimized by the Taguchi method", Journal of Applied Electrochemistry, 2011, 41, 19-27.

20. BabicÂ, R., MetikosÏ-HukovicÂ, M. and LoncÏar, M., "Impedance and photoelectrochemical study of surface layers on Cu and Cu-10Ni in acetate solution containing benzotriazole.", Electrochimica Acta., 1999, 44, 2413-2421.
21. Gerengi, H., Darowicki, K., Bereket, G., Slepski, P., "Evaluation of corrosion inhibition of brass-118 in artificial seawater by benzotriazole using Dynamic EIS", Corrosion Science, 2009, 51, p 2573–2579
22. Nam, N. D., M. J., Kim, Jang, Y. W. and Kim, J., G., "Effect of tin on the corrosion behavior of low-alloy steel in an acid chloride solution.", Corrosion Science., 2010, 52, 14-20.
23. Chase, W., Th., Notis, M. and Pelton, A., "Pourbaix (Eh-pH or EpH) Diagrams and Archaeological Corrosion of Bronzes, BUMA VI, Beijing, Sep. 15, 2006.